JBC RESEARCH ARTICLE

Phosphorylation of the RB C-terminus regulates condensin II release from chromatin

Received for publication, October 21, 2020 Published, Papers in Press, November 20, 2020, https://doi.org/10.1074/jbc.RA120.016511

Seung J. Kim[1,2,3], **James I. MacDonald**[1,2,4], **and Frederick A. Dick**[1,2,4,*]

From the [1]*London Regional Cancer Program and* [2]*Children's Health Research Institute, Lawson Health Research Institute, London, Ontario, Canada; and* [3]*Department of Biochemistry, and* [4]*Department of Pathology and Laboratory Medicine, Western University, London, Ontario, Canada*

Edited by Peter Cresswell

The retinoblastoma tumor suppressor protein (RB) plays an important role in biological processes such as cell cycle control, DNA damage repair, epigenetic regulation, and genome stability. The canonical model of RB regulation is that cyclin-CDKs phosphorylate and render RB inactive in late G1/S, promoting entry into S phase. Recently, monophosphorylated RB species were described to have distinct cell-cycle-independent functions, suggesting that a phosphorylation code dictates diversity of RB function. However, a biologically relevant, functional role of RB phosphorylation at non-CDK sites has remained elusive. Here, we investigated S838/T841 dual phosphorylation, its upstream stimulus, and downstream functional output. We found that mimicking T-cell receptor activation in Jurkat leukemia cells induced sequential activation of downstream kinases including p38 MAPK and RB S838/T841 phosphorylation. This signaling pathway disrupts RB and condensin II interaction with chromatin. Using cells expressing a WT or S838A/T841A mutant RB fragment, we present evidence that deficiency for this phosphorylation event prevents condensin II release from chromatin.

The retinoblastoma tumor suppressor protein (RB) is well characterized for its role in regulating entry into the cell cycle, and this is its canonical function. In G1, RB is bound to E2F transcription factors, repressing their ability to express cell cycle target genes (1, 2). Upon growth stimulation, cyclin D accumulates and binds to cyclin-dependent-kinases 4/6 (CDK4/6). Cyclin D-CDK4/6 complexes phosphorylate RB, partially relieving E2F repression (3). This leads to expression of cyclin E, and cyclin E-bound CDK2 hyperphosphorlyates RB. Hyperphosphorylated RB is thought to be inactivated, and free E2F transcription factors drive gene expression required for subsequent cell cycle progression (4–6).

This model, however, represents only one facet of RB function, and CDK-independent roles are emerging. These noncanonical functions are ascribed to a pool of chromatin-bound RB that localizes to various parts of the genome. For example, RB is required for recruiting DNA repair machinery for nonhomologous end joining (NHEJ) and homology-directed repair (HR) pathways at double-strand breaks (DSBs) (7, 8). In addition, RB recruits epigenetic writers to repetitive elements that deposit repressive histone marks (9, 10). Heterochromatinization of repetitive elements may be required to silence their transcription to avoid an autoimmune response and maintain chromosome stability (10–13). In particular, RB-dependent maintenance of histone 4 lysine 20 tri-methylation (H4K20me3) at pericentromeric repeats is required for proper chromatid segregation in anaphase (10). Furthermore, disrupting RB interaction with structural maintenance of chromatin containing complexes such as condensin II at pericentromeric repeats results in mitotic errors, replication defects, and aneuploidy (14, 15). Therefore, existing literature suggests that there is a pool of RB that is resistant to CDK inactivation and binds chromatin to carry out cell-cycle-independent functions.

Mechanistically, posttranslational modifications regulate RB's diverse functions (16). Notably, phosphorylation of RB can regulate its cell-cycle-independent functions. For example, CDK4/6 phosphorylation of RB at S249/T252 allows RB to bind and inactivate the NFκB family protein p65 and its immune-suppressive transcriptional program in prostate cancer cells (17). In addition, stress-induced p38 mitogen-activated protein kinase (MAPK) activation phosphorylates RB at S249/T252 to negate inactivation by CDKs and prevent cell cycle entry (18). Furthermore, monophosphorylation of RB at its 13 CDK phosphorylation sites confers ability to activate distinct transcriptional programs beyond cell cycle genes such as inflammatory response and mitochondrial oxidative phosphorylation (19). However, these studies have primarily focused on phosphorylation at CDK consensus sites, and RB phosphorylation at non-CDK sites and their functional outcomes are not fully characterized. Upon apoptotic stimulation, p38 MAPK, but not CDKs, phosphorylates RB at non-CDK sites and activates E2F1 transcription in a reporter assay (20). Specific non-CDK phosphorylation sites and their relevance to cellular function remain to be elucidated.

Here, we characterize RB phosphorylation on S838 and T841 (S838/T841) as a mechanistic link between T-cell receptor (TCR) activation and chromatin decondensation in Jurkat T-cells. Prompted by existing phospho-proteomic data, we generated an antibody specific to phosphorylation at S838/T841. We show that p38 MAPK is an upstream kinase that induces RB phosphorylation at these sites upon stimulus that

* For correspondence: Frederick A. Dick, fdick@uwo.ca.

mimics TCR activation in culture. Finally, we demonstrate that inability to phosphorylate these sites leads to defective condensin II release from chromatin.

Results

Detection of C-terminal RB phosphorylation on S838 and T841

Multiple residues located throughout RB are phosphorylated, and the functional roles of CDK sites have been extensively characterized. Many of these modifications serve to inactivate its canonical function of negatively regulating cell cycle entry through E2F transcription factor binding. Interestingly, RB monophosphorylation of CDK sites has been shown to activate specific molecular functions of RB that may extend beyond cell cycle control (19). We sought to identify RB phosphorylation at new sites and determine their roles in RB regulation.

Figure 1*A* depicts the open reading frame of RB, its known CDK phosphorylation sites (top), and potential phospho-acceptor residues that are uncharacterized (bottom). We focused on RB C-terminus (RBC) as it forms an α-helix, and any phosphorylation within this region is likely to disrupt protein–protein interactions, leading to a novel functional outcome. To identify candidate phosphorylation sites for our investigation, we curated predicted phosphorylation events within tryptic fragments corresponding to RBC from available phospho-proteomic data in different cells or tissues upon

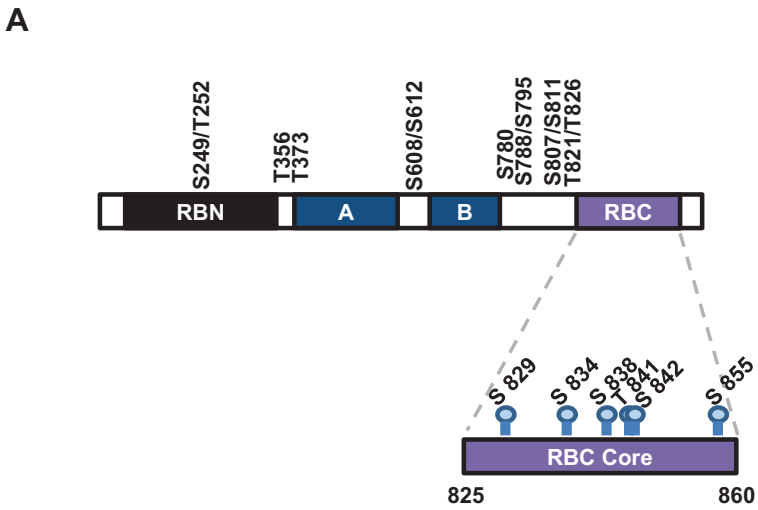

B

Study	Cell/Tissue	Treatment	S829	S834	S838	T841	S842	S855
Dephoure et al.	HeLa	Nocodazole						
Hoffert et al.	Kidney	CA and dDAVP						
Huttlin et al.	Spleen							
Kettenbach et al.	HeLa	Taxol						
Mayya et al.	Jurkat	TCR cross-link						
Mertins et al.	Jurkat	Bortezomib						
Sharma et al.	HeLa	Noc or EGF						
Zhou et al.	HeLa/K562							
CST A (15 studies)	Jurkat	PVA/CA						
CST B (2 studies)	Jurkat							
CST C (2 studies)	Jurkat	TPA						
CST D (3 studies)	Jurkat	PVA						
CST E (1 study)	K562							

Figure 1. Putative phosphorylation of the RB C-terminus. *A*, the open reading frame for RB is shown depicting known CDK phosphorylation sites (*top*) and uncharacterized, non-CDK phosphorylation sites in RBC (*bottom*). RB N-terminal domain (RBN), *A* and *B* halves of the pocket domain, and RB C-terminal domain (RBC) are shown. *B*, chart displaying potential phosphorylation sites in the amino acid 825 to 860 region of the RB C-terminus. Putative phosphorylation sites identified in publicly available phosphoproteomic studies are shaded in blue and the relevant data sources are indicated. CST, Cell Signaling Technologies data set.

various treatments (Fig. 1*B*) (21–29). A positive prediction for each serine or threonine residue is shaded in blue.

The phospho-proteomic data reveal that various combinations of serine and threonine residues within RBC are readily phosphorylated, supporting the idea that the RB phosphorylation "code" is yet incomplete. There is significant variability between the data sets on which exact sites are phosphorylated. This may indicate that complex, differential phosphorylation events occur in RBC depending on the cell type and stimulus, or that whole cell proteomics cannot accurately discern between neighboring phosphorylation events. While all of these potential modifications can be found in untreated cells, we focused on S838 and T841 phosphorylation because it is inducible upon TCR activation, a relevant signaling pathway in Jurkat leukemic T-cells.

In order to study S838 and T841 phosphorylation on RB further, we sought to generate a specific antibody for these modifications. We generated rabbit antiserum against an RB-derived peptide corresponding to amino acids 834 to 845, phosphorylated on S838 and T841. An ELISA was performed to confirm the specificity of our antibodies following purification from the antiserum. We found that anti-RB pS838/pT841antibodies had a tenfold higher affinity for the S838/T841 phosphorylated RB peptide than its unphosphorylated counterpart (Fig. 2*A*). Next, we sought to find evidence for RB phosphorylation on S838/T841 *in vitro* as predicted by phospho-proteomic data. We incubated glutathione S-transferase-tagged RBC (GST-RBC) with whole cell extract (Ext) from Jurkat cells treated with phosphatase inhibitors pervanadate and calyculin A (PVA/CA) to globally activate kinases that may phosphorylate RB. We found a time-dependent increase in RB S838/T841 phosphorylation in the presence of ATP (Fig. 2*B*). To account for the possibility that our antibody cross-reacts with other phosphorylation events in RBC (amino acids 792–928), we repeated the experiment with GST-RBC where S838 and T841 were substituted to alanine either together or as single mutants. This reveals that this antibody requires either S838 or T841 phosphorylation, but not both (Fig. 2*C*). For this reason, we describe the antibodies and detected phosphorylation events throughout this paper as pS838/pT841 because phosphorylation of either site alone, or both in combination, is possible. With the specificity of our antibody established, we determined if endogenous RB is phosphorylated on S838/T841. We treated Jurkat cells with PVA/CA to activate kinases and RB phosphorylation, prepared nuclear extracts (NE), and immunoblotted with our antibody. RB phosphorylation on S838/T841 was increased upon PVA/CA treatment, but it was also evident that our antibody cross-reacted with approximately six or seven proteins other than RB (Fig. 2*D*). To ensure we were certain of RB's identity, we repeated the cell treatment and immunoprecipitated total RB from Jurkat NE and performed an immunoblot with anti-RB pS838/pT841antibodies. Once again, we confirmed that RB phosphorylation on S838/T841 was induced upon PVA/CA treatment (Fig. 2*E*). In all subsequent experiments, we first immunoprecipitated RB, then probed with the antibody to assess S838/T841 phosphorylation.

These data demonstrate that our antibody is highly specific for phosphorylation within RBC, namely on S838/T841. Although it cross-reacts with a small number of nuclear proteins, first enriching for RB by immunoprecipitation is a robust and specific means of detecting phosphorylation of these sites. More importantly, we have shown the first line of evidence that S838/T841 phosphorylation is a *bona fide* RB post-translational modification that has not yet been studied functionally.

Sequential activation of kinases in the TCR signaling pathway induces RB S838/T841 phosphorylation

As a first step to understanding the functional role for RB S838/T841 phosphorylation, we sought to identify the kinase that was responsible for this modification. p38 MAPK has been shown to phosphorylate RB even when CDK sites are mutated (20). Therefore, we pretreated Jurkat cells with a p38 inhibitor, SB203580, then stimulated phosphorylation with PVA/CA. We found that SB203580 pretreatment strongly reduced RB S838/T841 phosphorylation despite PVA/CA treatment (Fig. 3*A*). As a positive control for p38 inhibition, we also measured phosphorylation of a known p38 target, MAPKAPK-2, and found that phosphorylation of its activation loop at T334 was also reduced. Next, we determined if immunoprecipitated p38 can phosphorylate RB at S838/T841 *in vitro*. We first isolated p38 by immunoprecipitating the active form with anti-p38 pT180/pY182 phosphorylation-specific antibodies. It was then incubated with GST-RBC in the presence or absence of its inhibitor. p38 phosphorylation of RB increased over time, and its inhibitor largely abrogated this effect (Fig. 3*B*).

These experiments strongly suggest that RB phosphorylation at S838/T841 is dependent on p38. PVA/CA treatment indiscriminately activates kinases, yet selective inhibition of p38 was sufficient to reduce RB phosphorylation to background level. Furthermore, partially purified, active p38 was necessary and sufficient to induce RB phosphorylation *in vitro* suggesting it may do so directly.

PVA/CA treatment has served as a way to easily and efficiently induce phosphorylation of RB. However, this treatment activates many pathways and hence does not offer insight into specific stimuli that induce RB S838/T841 phosphorylation under physiological conditions. Since p38 is a downstream target of T-cell receptor (TCR) signaling, and Jurkat cells are leukemic T-cells, we hypothesized that TCR activation phosphorylates RB through p38. We mimicked TCR activation by treating cells with an antibody cocktail that physically aggregates TCR and its costimulatory receptor together, as previously reported (30, 31). We then detected phosphorylation-dependent activation of proteins in the signaling pathway by immunoblotting. We observed rapid activation of ZAP70 within the first 5 min of antibody cross-linking and peak activation of p38 soon after at 15 min (Fig. 4*A*). TCR activation reproducibly induced p38 activation within the first 30 min (Fig. 4*B*). At 30 min we immunoprecipitated RB and found strong S838/T841 phosphorylation (Fig. 4*C*). In addition, TCR activation did not induce additional

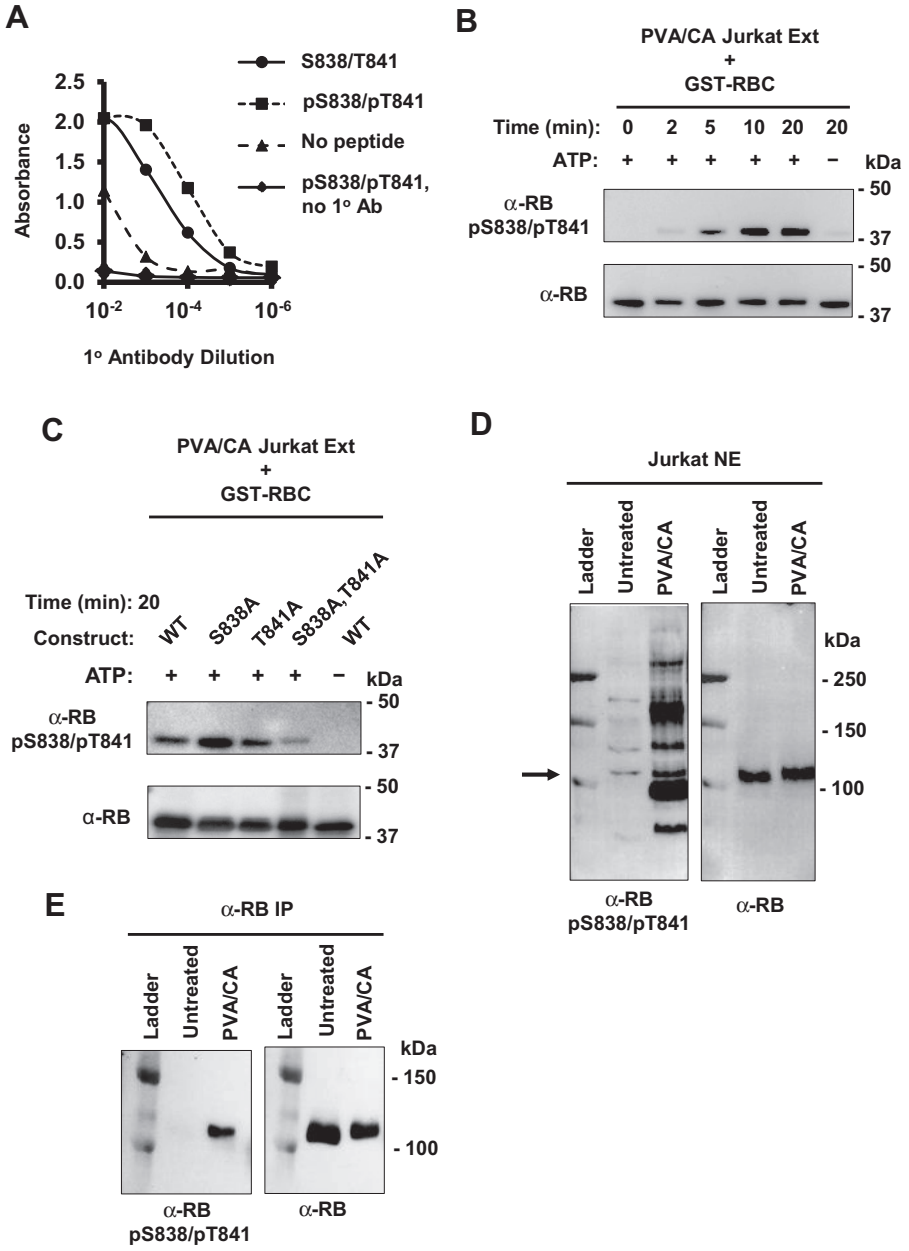

Figure 2. Detection of phosphorylation of S838/T841 on RB. *A*, rabbit antiserum was generated by immunizing animals with a peptide phosphorylated at S838 and T841. Phosphorylation-specific antibodies were purified and an ELISA was performed to determine their specificity. Phosphorylated or unphosphorylated peptides were adhered to microplate wells and incubated with anti-RB pS838/pT841antibodies. Control wells contained either no peptide or no antibody. Antibody binding was measured colorimetrically and graphed. *B*, a GST-tagged RBC fragment (aa 792–928) was incubated with PVA/CA-treated Jurkat whole cell extract for the indicated times, and omission of ATP was used as a negative control. Phosphorylation status was determined by immunoblotting with the anti-RB pS838/pT841, and blotting with anti-RB antibodies was used as a loading control. *C*, WT or mutant GST-RBC proteins were incubated with PVA/CA-treated Jurkat extracts with or without ATP for 20 min. Phosphorylation status was measured as in *B*. *D*, S838/T841 phosphorylation of endogenous RB was detected by western blotting with anti-RB pS838/pT841 antibodies in PVA/CA-treated Jurkat nuclear extracts (NE). This membrane was stripped and reprobed for RB, and the *arrow* indicates the corresponding RB band. *E*, jurkat cells were treated with PVA/CA, and RB was immunoprecipitated from NE with an α-RB antibody-coupled to Protein G Dynabeads. Phosphorylation status of S838/T841 was determined by western blotting.

phosphorylation of neighboring CDK phosphorylation sites, S807 and S811 consistent with these cells already being in a proliferative state. S838/T841 phosphorylated RB also retained its interaction with E2F1 and E2F2 as they were comparably coimmunoprecipitated relative to untreated cells. The shift in E2F2 migration upon TCR activation is consistent with previous proteomic data that report S117/S123 phosphorylation in Jurkat cells upon PVA/CA or TCR activation (25, 29).

These experiments implicate TCR activation as a relevant mechanism that induces RB S838/T841 phosphorylation and suggests that RB S838/T841 phosphorylation may regulate its noncanonical functions. Our antibody cocktail treatment appears to closely mimic TCR activation as both ZAP70 and p38 were activated sequentially in the anticipated order. A slight temporal delay in peak phosphorylation of ZAP70, p38, and ultimately RB also suggests that this signaling cascade is

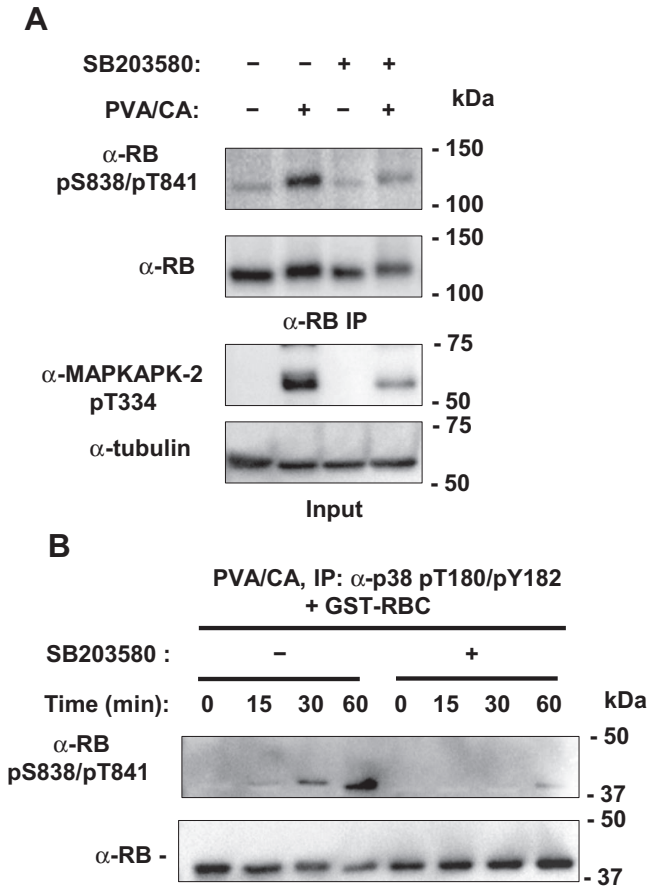

Figure 3. Phosphorylation of RB on S838/T841 is dependent on p38. *A*, jurkat cells were treated with PVA/CA with or without 10 μM SB203580, a p38 inhibitor. RB was immunoprecipitated from lysates with an α-RB antibody bound to Protein G Dynabeads, and phosphorylation of S838/T841 was detected by immunoblotting. As a positive control for p38 inhibition, phosphorylation of a known p38 phosphorylation target, T334 on MAPKAPK-2, was detected by western blotting. *B*, jurkat cells were treated with PVA/CA, and active p38 was immunoprecipitated from whole cell lysates with α-p38 pT180/pY182 antibodies bound to Protein G Dynabeads. Immunoprecipitated p38 was resuspended in kinase buffer containing GST-RBC, with or without 50 μM SB203580 for the indicated amount of time. Phosphorylation of S838/T841 and GST-RBC was detected by western blotting as indicated.

biologically relevant to TCR activation. Furthermore, because S838/T841 phosphorylation in response to TCR signaling is unlinked to CDK phosphorylation, its function is unlikely to be related to cell cycle entry or control of E2F-dependent transcription.

RB S838/T841 phospho-acceptor mutants prevent condensin II unloading and chromatin decondensation

The majority of previously described RB function stems from its ability to occupy chromatin. For example, RB protects genome integrity during mitosis by recruiting the condensin II complex to pericentromeric heterochromatin (15). In addition, the condensin II complex has a role in developing T-cells. The *nessy* mutant allele of CAPH2, one of the subunits of the complex, results in defective condensation of T-cell chromatin and development (32, 33). Since RB is phosphorylated under conditions that mimic TCR signaling, and is known to recruit condensin II to chromatin, we hypothesized that RB S838/T841 phosphorylation may regulate RB–condensin II interactions on chromatin in T-cells.

In order to compare chromatin occupancy upon TCR cross-linking, we first sought to establish that this stimulus did not affect total expression of the proteins of interest. Indeed, we confirmed that expression of CAPH2, RB, E2F1, and SMC1, a cohesin subunit, was not changed in whole cell extracts (Fig. 5*A*, left). However, TCR cross-linking for 30 min induced release of RB, E2F1, and CAPH2, but not SMC1 from chromatin (Fig. 5*A*, right). Using densitometric analysis of these experiments, we found that TCR cross-linking released 40% of CAPH2 from chromatin (Fig. 5*B*). To examine the precise role of S838/T841 phosphorylation in this process, we created a phospho-acceptor mutation in RB with a S838A/T841A double alanine substitution. To stably express this mutant in cells, we generated lentiviral vectors coding for HA-tagged large pocket fragment of RB (RBLP, amino acids 379–928). Jurkat cells were transduced with lentiviruses expressing either the WT RBLP (RBLP-WT) or S838A/T841A (RBLP-AA) construct (Fig. 5*C*). We confirmed equivalent expression of both constructs by immunoblotting for the HA-tag (Fig. 5*D*). We cross-linked TCRs as before and investigated CAPH2 and SMC1 chromatin levels (Fig. 5*E*). This revealed that RBLP-AA expressing cells retained similar levels of chromatin-bound CAPH2 as unstimulated cells and that RBLP-WT expressing cells released CAPH2 similarly to untransduced Jurkat cells (Fig. 5*E*). We normalized CAPH2 release to SMC1-bound chromatin levels to quantitate the inhibition of CAPH2 release by RBLP-AA (Fig. 5*F*). These experiments confirm that the inability to phosphorylate RB at S838/T841 dominantly blocks condensin II release from chromatin.

Next, we sought to describe a biochemical consequence of defective CAPH2 unloading. To assess changes in chromatin structure upon TCR cross-linking, we used sensitivity to sonication-induced chromatin shearing as a readout for chromatin compaction as previously reported (Fig. 6*A*) (33). Untreated or TCR cross-linked cells were fixed to immobilize DNA–protein contacts and fractionated to obtain total chromatin. Isolated chromatin was sheared by a range of sonication cycles, and the presence of high-molecular-weight DNA fragments was detected by agarose gel electrophoresis and ethidium bromide staining. In line with Figure 5*A*, TCR cross-linking decreased the amount of high-molecular-weight DNA remaining after the same number of sonication cycles compared with control cells that were untreated (Fig. 6, *B–C*). We repeated this TCR cross-linking experiment using cells that express RBLP-WT or the -AA mutant. This revealed that chromatin isolated from RBLP-AA expressing cells was sheared less effectively compared with that from RBLP-WT expressing cells (Fig. 6, *D–E*). This suggests that the RB S838A/T841A mutant disrupts TCR cross-link-mediated chromatin decondensation and suggests that the phosphorylation of RB on these sites plays a key role in chromatin decondensation by releasing RB and condensin II from chromatin.

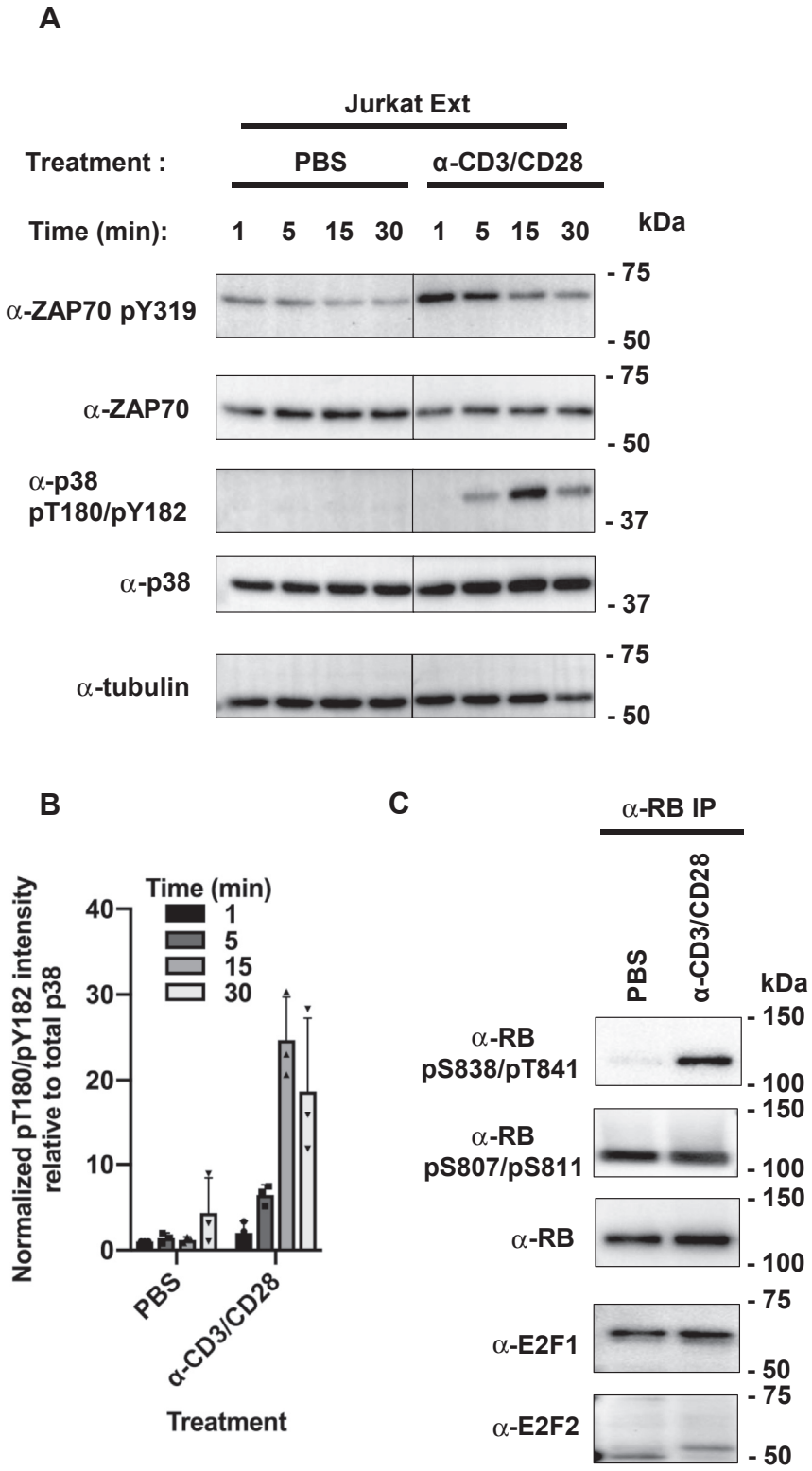

Figure 4. T-cell receptor signaling causes RB S838/T841 phosphorylation. *A*, jurkat cells were treated with PBS, or anti-CD3, anti-CD28, and a secondary antibody to cross-link T-cell receptors for the indicated time points. Each time point was quenched by washing cells with cold PBS and immediately lysed to generate whole cell extracts. Abundance of phosphorylated species relative to total ZAP70 and p38 was determined with immunoblotting as a readout. Relevant lanes from a single whole image was spliced together at the vertical line in the center for each blot. *B*, jurkat cells were treated as in A for 30 min. RB was immunoprecipitated from whole cell extracts with α-RB antibodies bound to Protein G Dynabeads. RB phosphorylation on S838/T841 and S807/S811 was determined by blotting, and coimmunoprecipitating E2Fs were detected similarly.

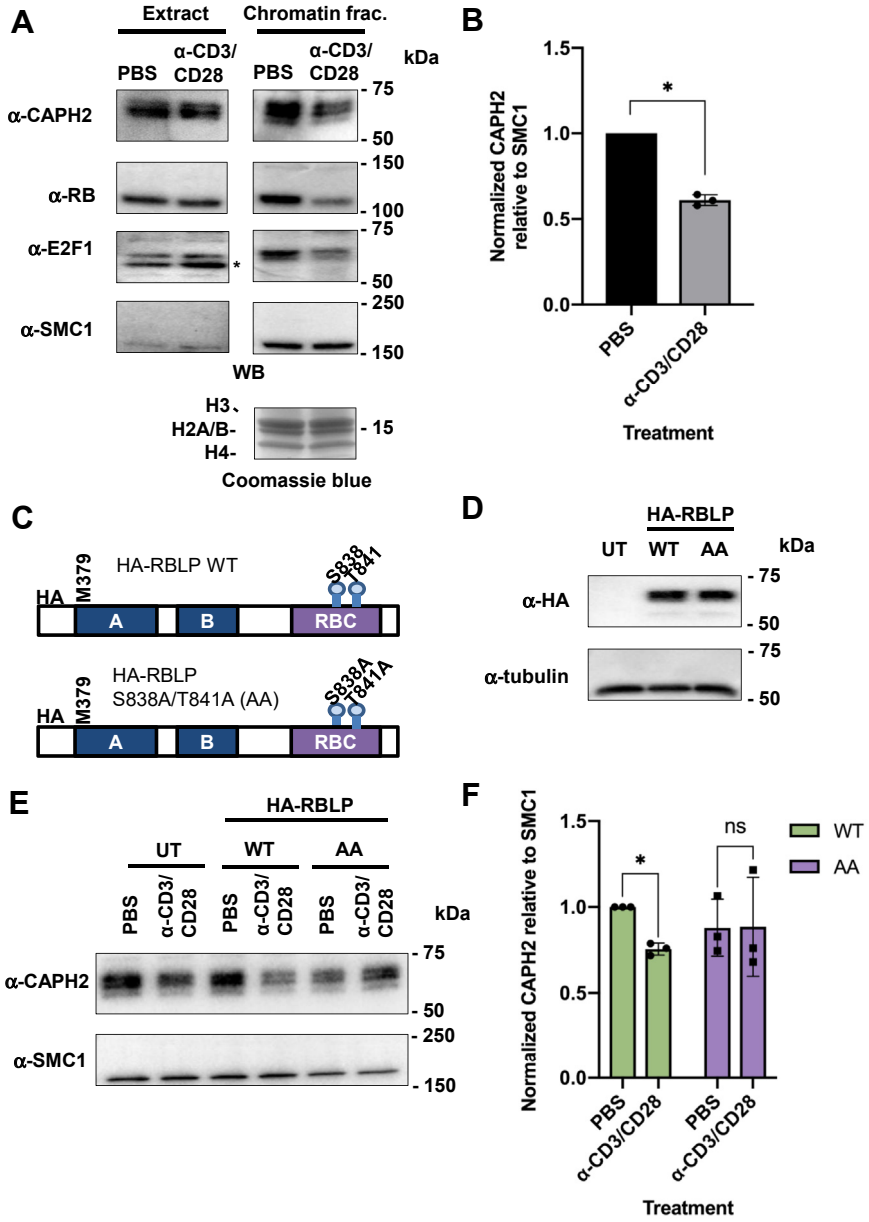

Figure 5. Nonphosphorylatable S838A/T841A RB prevents CAPH2 chromatin unloading upon T-cell receptor cross-linking. *A*, jurkat cells were treated as indicated for 30 min, whole cell extracts and chromatin fractions were prepared, and expression levels of the indicated proteins were detected by western blotting. Histone levels serve as loading control and were detected by Coomassie Blue staining. * indicates nonspecific band. *B*, relative levels of CAPH2 in chromatin fractions was normalized to SMC1 and compared between treated and untreated conditions (n = 3, * $p < 0.05$, Student's *t*-test). *C*, the open reading frame for WT and mutant RBLP constructs (aa 379–928) are shown depicting their relevant coding regions and HA tags. The mutant construct labeled RBLP AA carries double alanine substitutions at S838 and T841. *D*, lentiviruses were used to transduce RBLP and the AA mutant construct into Jurkat cells. Expression of exogenous RBLP was detected by western blotting for HA. Tubulin blots serve as loading controls. *E*, jurkat cells expressing either WT or RBLP, or untransduced controls (UT), were subjected to TCR cross-linking for 30 min. Chromatin fractions were prepared, and levels of the indicated proteins were detected by western blotting. *F*, levels of chromatin-associated CAPH2 were normalized to SMC1 and compared between PBS and TCR cross-linked conditions (n = 3, * $p < 0.05$, Two-way ANOVA and Sidak's multiple comparisons test).

Discussion

In this report, we characterized a functional role for non-CDK phosphorylation of RB. By curating existing phosphoproteomic data, we generated and validated S838/T841 phospho-specific antibodies. With this tool, we showed that p38 MAPK is an upstream kinase that can direct RB phosphorylation and that TCR cross-linking induces a signaling cascade that ultimately phosphorylates RB in Jurkat cells on these sites. To probe its mechanistic role, we generated cell lines that stably express phospho-acceptor mutant RB. Finally, our data demonstrates that when RB is unable to be phosphorylated at S838/T841, TCR signaling is unable to release condensin II from chromatin. This conclusion is consistent with previous work that describes RB–condensin II chromatin interactions and T-cell development and contributes to our understanding of an emerging RB phosphorylation code.

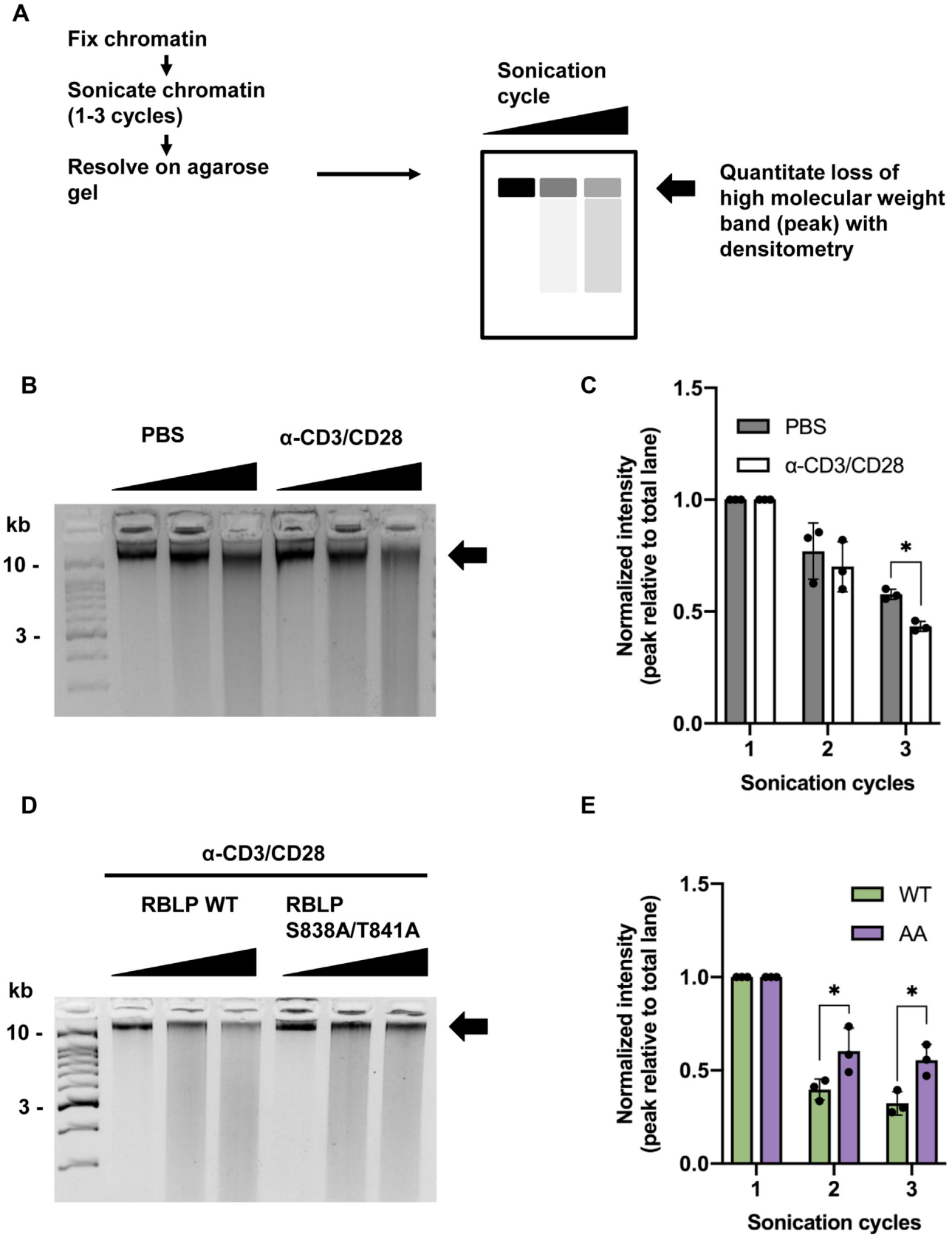

Figure 6. RB S838/T841 phosphorylation regulates chromatin dynamics upon T-cell receptor signaling. *A* jurkat cells were stimulated by T-cell receptor cross-linking as indicated. Cells were fixed and lysed to obtain chromatin fractions. Chromatin was sonicated for one to three cycles. Protein–DNA cross-links were reversed, and DNA was purified and analyzed on a 3% agarose gel. DNA was stained with ethidium bromide and visualized on a Chemi Doc. The high-molecular-weight DNA band indicated by the *arrow* was quantified on Image Lab, and intensity is expressed as a percentage of the total lane normalized within each group. *B*, untransduced Jurkat cells were PBS or TCR cross-linked as described in A. Chromatin fragmentation is shown. *C*, percent

TCR cross-linking induced marked loss of chromatin-bound CAP-H2, but not SMC1, suggesting large-scale, yet selective reorganization of chromatin architecture. Importantly, expression of RBLP-AA was sufficient to disrupt TCR cross-linking-induced CAP-H2 release. The selective nature of RB regulation of condensin II in Jurkat T-cells agrees with the previous characterization of the *nessy* mutant CAP-H2 allele that is responsible for defective T-cell differentiation. Recently published work may inform future studies on specific consequences of the release of CAP-H2 in this model. CAP-H2 and transcription factor IIIC (TFIIIC) localize to histone clusters in mouse embryonic stem cells and serve to maintain topologically associated domains that regulate transcription (34). In addition, RB-condensin II complexes can regulate transcription at bidirectional promoters and maintain long-range chromosomal interactions. ChIP-sequencing (ChIP-Seq) for condensin II and TFIIIC components upon TCR cross-linking may inform site-specific loss of interaction, and the mechanistic role of RB can be delineated with a phospho-acceptor RB mutant. For increased sensitivity, gene editing technologies should be adopted to mutate endogenous RB or deplete endogenous RB with an inducible system as previously reported. ChIP-seq data should be interpreted together with high-throughput chromosome conformation capture (3C) such as 4C-seq to fully characterize functional consequences.

We speculate that RB phosphorylation at S838/T841 may be a key step in naive T-cell activation. Previous work has demonstrated that chromatin condensation orchestrated by condensin II is required to avoid cell death in developing thymocytes (33). Once mature, these cells become quiescent. Upon TCR activation through cognate antigen binding and costimulation, re-entry into cell cycle is coupled with chromatin decondensation and nuclear expansion in naïve T-cells. Loss of CAP-H2 chromatin occupancy upon TCR cross-linking in Jurkat T-cells is in line with such macromolecular changes during T-cell activation. Furthermore, TCR cross-linking with CD3/CD28 antibodies specifically induced RB phosphorylation at S838/T841, but not at its CDK sites. RB interaction with E2F transcription factors was also unaffected. These data suggest that S838/T841 phosphorylation is functionally distinct from canonical cell cycle control by RB that may also be cell type specific. Future work with peripheral T-cells *ex vivo* is warranted to support this model.

Ultimately, our work adds a layer of complexity to phosphorylation-dependent regulation of RB function. The canonical model of cell cycle control by RB has been binary; cyclin-CDK-driven RB hyperphosphorylation renders RB's negative regulation of E2F transcription factors inactive. Recently, however, various monophosphorylated RB species at one of its CDK sites have been shown to regulate cell-cycle-independent transcription programs. We showed that cell-cycle-independent TCR cross-linking induces a signaling cascade *via* p38 that can ultimately phosphorylate RB at S838/T841. Future work is warranted to characterize the relevance and functional roles of S838/T841 phosphorylation in other physiological circumstances.

Experimental procedures

Antibodies

Anti-RB pS838/pT841 antibody was produced in rabbits by Covance (Pennsylvania, USA). The peptide immunogen corresponded to the sequence 834-SIGE(pS)FG(pT)SEKF-845 of pRB. Peptides were immobilized using the Sulfo-link coupling reagent (Thermo Fisher) following the manufacturer's recommendations. The phospho-specific antibody was purified using standard procedures by passing serum first over the nonphosphorylated peptide column and secondly over the phosphorylated-peptide column to remove any antibodies recognizing the nonphosphorylated species. Anti-RB pS838/pT841 antibody was used in primary antibody solution at 0.5 mg/ml for Western blotting. Anti-MAPKAPK-2 pT334 (27B7), p38 pT180/pY182 (9211), total p38 (9212), α-tubulin (11H10), and RB pS807/pS811 (9308) antibodies were obtained from Cell Signaling Technology. Anti-HA antibody (3F10) was from Sigma. Anti-pRB monoclonal antibody (G3-245) was from BD Pharmingen, pRB rabbit polyclonal antibodies and E2F1 antibody (C-20) were from Santa Cruz, CAP-H2 antibody (A302-275A) was from Bethyl Laboratories. Anti-rabbit or anti-mouse IgG goat antibody conjugated to HRP was from GE Healthcare. For TCR activation studies, anti-CD3ε (OKT3) and CD28 (CD28.2) antibodies were from BioLegend, and light chain-specific goat anti-mouse IgG (115-005-174) was from Jackson ImmunoResearch Labs.

Cell culture and stimulation

Suspension Jurkat cells were grown in DMEM enriched with 10% v/v FBS, L-glutamine, penicillin, and streptomycin at 37 °C in 5% CO_2. For SB203580 inhibitor pretreatment, Jurkat cells (10^7) were suspended in 5 ml enriched DMEM and SB203580 (Cell Signaling Technology) was added from 10 mM stock to a final concentration of 10 μM. Equal volume of DMSO was added to control samples. The cells were then incubated at 37 °C for 2 h until treatment with pervanadate and calyculin (PVA/CA). Cells were centrifuged at 300*g* for 5 min at 4 °C and washed twice with PBS. After the last wash, the pellet was resuspended in 5 ml enriched DMEM, and PVA/CA was added to a final concentration of 100 and 0.1 μM, respectively. Control samples received equal volumes of PBS and DMSO vehicles, respectively. Both groups were incubated at 37 °C for 20 min. TCR activation was achieved as previously described with modifications (21). Jurkat cells (5×10^6) were resuspended in 1 ml enriched media and treated with 5 μg/ml anti-CD3ε and CD28 antibodies and 30 μg/ml goat anti-mouse

high-molecular-weight DNA quantities were averaged and graphed (n = 3, * indicates $p < 0.05$, two-way ANOVA with Sidak's multiple comparisons test). *D*, lentiviral transduced Jurkat cells were stimulated by T-cell receptor cross-linking, fixed, and lysed to obtain chromatin fractions. Chromatin was sonicated for increasing number of cycles and analyzed as in *A*. *E*, the high-molecular-weight band indicated by the *arrow* was quantified, averaged, and graphed, (n = 3, * indicates $p < 0.05$, Two-way ANOVA with Sidak's multiple comparisons test).

IgG to cross-link the primary antibodies. The cells were then incubated for indicated times at 37 °C, after which they were harvested.

Protein extract preparation

All of the following lysis buffers were supplemented with 250 μM Na_3VO_4, 5 mM NaF, 1 mM PMSF, 5 μg/L aprotinin, and leupeptin immediately before use. For whole cell extract (Ext), cells were washed twice with cold PBS and resuspended in lysis buffer containing 25 mM Tris-Cl pH 7.5, 100 mM NaCl, 5% (v/v) glycerol, and 1% (v/v) NP-40 and incubated on ice for 10 min. Insoluble material was cleared by centrifugation at 12,000*g* at 4 °C for 10 min. For NE, cells were washed twice with cold PBS, resuspended in hypotonic lysis buffer containing 10 mM Tris-Cl pH 7.5, 10 mM KCl, 3 mM $MgCl_2$, 1 mM EDTA, and 0.05% (v/v) NP-40, and incubated on ice for 5 min. Nuclei were isolated by centrifuging the suspension at 1300*g* at 4 °C for 5 min. The pelleted nuclei were washed twice in the same buffer. The nuclei were lysed in buffer containing 20 mM Tris-Cl pH 7.5, 420 mM NaCl, 1.5 mM $MgCl_2$, 0.2 mM EDTA, 25% (v/v) glycerol, 0.1% (v/v) NP-40 and incubated on ice for 10 min. Insoluble material was cleared by centrifugation at 12,000*g* at 4 °C for 10 min. For chromatin fractionation, PBS washed cells were incubated for 10 min on ice in buffer containing 10 mM Tris-Cl pH 8.0, 10 mM KCl, 1.5 mM $MgCl_2$, 0.34 M sucrose, 10% (v/v) glycerol, and 0.1% (v/v) Triton X-100 to lyse outer membrane. Nuclei were isolated by centrifuging the suspension at 1300*g* at 4 °C for 5 min. The pelleted nuclei were washed twice in the same buffer without Triton X-100. The nuclei were lysed in buffer containing 3 mM EDTA and 0.2 mM EGTA for 30 min on ice with occasional mixing. Nucleoplasmic fraction was removed by centrifuging the lysate at 4000*g* at 4 °C for 5 min. Remaining chromatin fraction was solubilized with DNaseI treatment at 37 °C for 10 min in buffer containing 10 mM Tris-Cl, 2.5 mM $MgCl_2$, 0.5 mM $CaCl_2$. Protein concentration was quantified by Bradford assay following standard procedures.

Immunoprecipitation

Antibodies to RB or pp38 T180/Y182 were diluted 1:50 in Ext containing 1 to 2 mg total protein. The lysates were incubated at 4 °C overnight with gentle agitation. In total, 50 μl Dynabeads Protein G (Thermo Fisher) was added and incubated at 4 °C for 2 h with gentle agitation. A magnet was used to immobilize the beads and to discard the supernatant.

In vitro *kinase assay*

Immunoprecipitated pp38 T180/Y182-Dynabeads complexes were used in kinase assays similar to previous reports. The complexes were resuspended in 50 μl kinase buffer containing 25 mM Tris-Cl pH 7.5, 5 mM β-glycerophosphate, 10 mM $MgCl_2$, 0.25 mM Na_3VO_4, and 5 mM NaF. Each of the time points consisted of a 40 μl reaction containing 5 μl of immunoprecipitated kinase or WCE (where indicated), 10 μg of GST-RBC, 1 mM ATP, and 50 μM SB203580 (where indicated) in kinase buffer. GST fusion proteins were expressed in *E. coli* BL21 (DE3) and purified with Glutathione Sepharose 4B (Sigma) following the manufacturer's recommendation. The reactions were prepared on ice, then transferred to 37 °C to start the assay. After the given incubation times, the immunoprecipitated proteins were immobilized with a magnet, and the remaining supernatant was saved.

SDS-PAGE, immunoblotting, and Coomassie staining

Protein extracts, supernatants, and immunoprecipitated beads were diluted in SDS-PAGE sample buffer to a final concentration of 62.5 mM Tris-Cl pH 6.8, 10% glycerol, 2% SDS, 72.5 mM β-mercaptoethanol, and 0.005% bromophenol blue. SDS-PAGE was performed following standard procedures. After gel electrophoresis, proteins were transferred to PVDF membrane and incubated with primary antibodies diluted in 5% milk or BSA in TBS-T over night at 4 °C with gentle agitation. Membranes were washed five times in tris buffered saline-Tween 20 (TBS-T) for 5 min and incubated with horseradish peroxidase (HRP)-conjugated goat secondary antibody for 1 h at room temperature. Membranes were washed again, incubated in SuperSignal WestDura (Thermo Fisher) for 5 min protected from light, and developed on a ChemiDoc (Bio-rad). For Coomassie staining, gels were washed three times in water and incubated in GelCode Blue (Thermo Fisher) over night at room temperature with gentle agitation. Stained gels were washed again twice in water. Bands were imaged on a ChemiDoc.

Plasmids and lentiviral transduction

Briefly, pSicoR-Ef1a-mCh-Puro (Addgene #31845) was double-digested with AfeI and SmaI to replace mCherry coding sequence with that of RBLP with matching sticky ends in-frame. S838A/T841A substituted plasmid was made with QuikChange Site-directed mutagenesis kit (Agilent), following manufacturer's recommendations and mutagenic primers TTAGTATCAATTGGTGAAGCATTCGGGGCTTCTGAGAAGTTCCAGAAA and TTTCTGGAACTTCTCAGAAGCCCCGAATGCTTCACCAATTGATACTAA. HEK293 T cells at 70% confluency on 10-cm plates were transfected with 12 μg expression vector, 9 μg pMD2.G (Addgene #12259), and 3 μg psPAX2 (Addgene #12260) using Lipofectamine 3000 (Life Technologies) following manufacturer's recommendations. Two days later, the cell media was harvested and passed through a 0.45 μm filter. Jurkat cells (10^6) were transduced with the filtrate containing 8 μg/ml polybrene. Transduced Jurkat cells were maintained in 0.3 μg/ml puromycin.

Chromatin sonication

Jurkat cells were washed twice in PBS and fixed in 1% formaldehyde/PBS for 10 min at room temperature with gentle agitation. Fixation was quenched with 0.125 M glycine for 5 min at room temperature. Cells were washed twice in cold PBS and incubated for 10 min on ice in buffer containing 10 mM HEPES pH 6.5, 10 mM EDTA, 0.5 mM EGTA, and 0.25% Triton X-100. Nuclei were isolated by centrifuging the suspension at 600*g* at 4 °C for 5 min. The pelleted nuclei were

lysed and washed twice in buffer containing 10 mM HEPES pH 6.5, 10 mM EDTA, 0.5 mM EGTA, and 200 mM NaCl. Chromatin isolated from 3 million cells was resuspended in 300 μl of buffer containing 50 mM Tris-Cl pH 8.0, 1 mM EDTA, 0.5% Triton X-100, and 1% SDS and aliquoted into 1.5 ml microtubes (Diagenode). All of the above lysis buffers were supplemented with 250 μM Na_3VO_4, 5 mM NaF, 1 mM PMSF, 5 μg/L aprotinin, and leupeptin immediately before use. Chromatin was sonicated in Bioruptor Pico (Diagenode) at 4 °C with one to three cycles. Each cycle consisted of 15 s ON and 30 s OFF. After sonication, chromatin–protein complexes were reverse-cross-linked by adding NaCl to a final concentration of 200 mM to each sample and incubating overnight at 65 °C. RNA and protein were removed by RNase A and proteinase K digestion, respectively. DNA was isolated by phenol-chloroform extraction and ethanol precipitation and analyzed on 3% agarose gels. DNA was stained with ethidium bromide and visualized on a Chemi Doc. High-molecular-weight DNA bands were quantified as a percentage of the total lane intensity with lower threshold cutoff at 100 bp using Image Lab 5.2.

Statistical analysis

All statistical analyses were performed on Prism 8. CAPH2 chromatin loading relative to SMC1 in untransduced cells was compared using Student's *t*-test. That of HA-RBLP WT or AA expressing cells was compared using two-way ANOVA and Sidak's multiple comparisons test. For sonicated chromatin densitometry, the mean of triplicate values was compared between treatment conditions, or cell lines, as indicated by two-way ANOVA. Sidak's multiple comparison test was used.

Data availability

All data are contained within the manuscript.

Acknowledgments—The authors wish to thank colleagues at the London Regional Cancer Program for suggestions and encouragement in the course of this work.

Author contributions—S. J. K. carried out all experiments except Figure 2*A*, *B*, *D*, and *E*. J. I. M. carried out experiments in Figure 2*A*, *B*, *D*, and *E*. S. J. K. and F. A. D. wrote the manuscript.

Funding and additional information—S. J. K. was funded by Cancer Research and Technology Transfer training program and Ontario Graduate Scholarship. This work was supported by a grant from the Cancer Research Society. F. A. D. is the Wolfe Senior Fellow in Tumor Suppressor Genes at Western University.

Conflict of interest—The authors declare that they have no conflicts of interest with the contents of this article.

Abbreviations—The abbreviations used are: CA, calyculin A; CDK, cyclin-dependent kinase; DSB, double-strand break; Ext, whole cell extract; GST, glutathione S-transferase; HA, hemagglutinin; MAPK, mitogen-activated protein kinase; NHEJ, nonhomologous end joining; PVA, pervanadate; RB, retinoblastoma tumor suppressor protein; RBC, RB C-terminus; RBLP, RB large pocket; TCR, T-cell receptor.

References

1. Weinberg, R. A. (1995) The retinoblastoma protein and cell cycle control. *Cell* **81**, 323–330
2. Chellappan, S. P., Hiebert, S., Mudryj, M., Horowitz, J. M., and Nevins, J. R. (1991) The E2F transcription factor is a cellular target for the RB protein. *Cell* **65**, 1053–1061
3. Lundberg, A. S., and Weinberg, R. A. (1998) Functional inactivation of the retinoblastoma protein requires sequential modification by at least two distinct cyclin-cdk complexes. *Mol. Cell. Biol.* **18**, 753–761
4. DeGregori, J., Leone, G., Miron, A., Jakoi, L., and Nevins, J. R. (1997) Distinct roles for E2F proteins in cell growth control and apoptosis. *Proc. Natl. Acad. Sci. U. S. A.* **94**, 7245–7250
5. Dyson, N. (1998) The regulation of E2F by pRB-family proteins. *Genes Dev.* **12**, 2245–2262
6. Mittnacht, S. (1998) Control of pRB phosphorylation. *Curr. Opin. Genet. Dev.* **8**, 21–27
7. Cook, R., Zoumpoulidou, G., Luczynski, M. T., Rieger, S., Moquet, J., Spanswick, V. J., Hartley, J. A., Rothkamm, K., Huang, P. H., and Mittnacht, S. (2015) Direct involvement of retinoblastoma family proteins in DNA repair by non-homologous end-joining. *Cell Rep.* **10**, 2006–2018
8. Vélez-Cruz, R., Manickavinayaham, S., Biswas, A. K., Clary, R. W., Premkumar, T., Cole, F., and Johnson, D. G. (2016) RB localizes to DNA double-strand breaks and promotes DNA end resection and homologous recombination through the recruitment of BRG1. *Genes Dev.* **30**, 2500–2512
9. Ishak, C. A., Marshall, A. E., Passos, D. T., White, C. R., Kim, S. J., Cecchini, M. J., Ferwati, S., MacDonald, W. A., Howlett, C. J., Welch, I. D., Rubin, S. M., Mann, M. R. W., and Dick, F. A. (2016) An RB-EZH2 complex mediates silencing of repetitive DNA sequences. *Mol. Cell* **64**, 1074–1087
10. Manning, A. L., Yazinski, S. A., Nicolay, B., Bryll, A., Zou, L., and Dyson, N. J. (2014) Suppression of genome instability in pRB-deficient cells by enhancement of chromosome cohesion. *Mol. Cell* **53**, 993–1004
11. Rajshekar, S., Yao, J., Arnold, P. K., Payne, S. G., Zhang, Y., Bowman, T. V., Schmitz, R. J., Edwards, J. R., and Goll, M. (2018) Pericentromeric hypomethylation elicits an interferon response in an animal model of ICF syndrome. *Elife* **7**, e39658
12. Chiappinelli, K. B., Strissel, P. L., Desrichard, A., Li, H., Henke, C., Akman, B., Hein, A., Rote, N. S., Cope, L. M., Snyder, A., Makarov, V., Buhu, S., Slamon, D. J., Wolchok, J. D., Pardoll, D. M., *et al.* (2015) Inhibiting DNA methylation causes an interferon response in cancer via dsRNA including endogenous retroviruses. *Cell* **162**, 974–986
13. Roulois, D., Loo Yau, H., Singhania, R., Wang, Y., Danesh, A., Shen, S. Y., Han, H., Liang, G., Jones, P. A., Pugh, T. J., O'Brien, C., and De Carvalho, D. D. (2015) DNA-demethylating agents target colorectal cancer cells by inducing viral mimicry by endogenous transcripts. *Cell* **162**, 961–973
14. Longworth, M. S., Herr, A., Ji, J.-Y., and Dyson, N. J. (2008) RBF1 promotes chromatin condensation through a conserved interaction with the condensin II protein dCAP-D3. *Genes Dev.* **22**, 1011–1024
15. Coschi, C. H., Ishak, C. A., Gallo, D., Marshall, A., Talluri, S., Wang, J., Cecchini, M. J., Martens, A. L., Percy, V., Welch, I., Boutros, P. C., Brown, G. W., and Dick, F. A. (2014) Haploinsufficiency of an RB-E2F1-condensin II complex leads to aberrant replication and aneuploidy. *Cancer Discov.* **4**, 840–853
16. MacDonald, J. I., and Dick, F. A. (2012) Posttranslational modifications of the retinoblastoma tumor suppressor protein as determinants of function. *Genes Cancer* **3**, 619–633
17. Jin, X., Ding, D., Yan, Y., Li, H., Wang, B., Ma, L., Ye, Z., Ma, T., Wu, Q., Rodrigues, D. N., Kohli, M., Jimenez, R., Wang, L., Goodrich, D. W., de Bono, J., *et al.* (2019) Phosphorylated RB promotes cancer immunity by inhibiting NF-κB activation and PD-L1 expression. *Mol. Cell* **73**, 22–35.e6

18. Gubern, A., Joaquin, M., Marquès, M., Maseres, P., Garcia-Garcia, J., Amat, R., González-Nuñez, D., Oliva, B., Real, F. X., de Nadal, E., and Posas, F. (2016) The N-terminal phosphorylation of RB by p38 bypasses its inactivation by CDKs and prevents proliferation in cancer cells. *Mol. Cell* **64**, 25–36
19. Sanidas, I., Morris, R., Fella, K. A., Rumde, P. H., Boukhali, M., Tai, E. C., Ting, D. T., Lawrence, M. S., Haas, W., and Dyson, N. J. (2019) A code of mono-phosphorylation modulates the function of RB. *Mol. Cell* **73**, 985–1000.e6
20. Nath, N., Wang, S., Betts, V., Knudsen, E., and Chellappan, S. (2003) Apoptotic and mitogenic stimuli inactivate Rb by differential utilization of p38 and cyclin-dependent kinases. *Oncogene* **22**, 5986–5994
21. Dephoure, N., Zhou, C., Villen, J., Beausoleil, S. A., Bakalarski, C. E., Elledge, S. J., and Gygi, S. P. (2008) A quantitative atlas of mitotic phosphorylation. *Proc. Natl. Acad. Sci. U. S. A.* **105**, 10762–10767
22. Hoffert, J. D., Pisitkun, T., Wang, G., Shen, R.-F., and Knepper, M. A. (2006) Quantitative phosphoproteomics of vasopressin-sensitive renal cells: regulation of aquaporin-2 phosphorylation at two sites. *Proc. Natl. Acad. Sci. U. S. A.* **103**, 7159–7164
23. Huttlin, E. L., Jedrychowski, M. P., Elias, J. E., Goswami, T., Rad, R., Beausoleil, S. A., Villén, J., Haas, W., Sowa, M. E., and Gygi, S. P. (2010) A tissue-specific atlas of mouse protein phosphorylation and expression. *Cell* **143**, 1174–1189
24. Kettenbach, A. N., Schweppe, D. K., Faherty, B. K., Pechenick, D., Pletnev, A. A., and Gerber, S. A. (2011) Quantitative phosphoproteomics identifies substrates and functional modules of aurora and polo-like kinase activities in mitotic cells. *Sci. Signal.* **4**, rs5
25. Mayya, V., Lundgren, D. H., Hwang, S.-I., Rezaul, K., Wu, L., Eng, J. K., Rodionov, V., and Han, D. K. (2009) Quantitative phosphoproteomic analysis of T cell receptor signaling reveals system-wide modulation of protein-protein interactions. *Sci. Signal.* **2**, ra46
26. Mertins, P., Qiao, J. W., Patel, J., Udeshi, N. D., Clauser, K. R., Mani, D. R., Burgess, M. W., Gillette, M. A., Jaffe, J. D., and Carr, S. A. (2013) Integrated proteomic analysis of post-translational modifications by serial enrichment. *Nat. Methods* **10**, 634–637
27. Sharma, K., D'Souza, R. C. J., Tyanova, S., Schaab, C., Wiśniewski, J. R., Cox, J., and Mann, M. (2014) Ultradeep human phosphoproteome reveals a distinct regulatory nature of Tyr and Ser/Thr-based signaling. *Cell Rep.* **8**, 1583–1594
28. Zhou, H., Di Palma, S., Preisinger, C., Peng, M., Polat, A. N., Heck, A. J. R., and Mohammed, S. (2013) Toward a comprehensive characterization of a human cancer cell phosphoproteome. *J. Proteome Res.* **12**, 260–271
29. Hornbeck, P. V., Kornhauser, J. M., Tkachev, S., Zhang, B., Skrzypek, E., Murray, B., Latham, V., and Sullivan, M. (2012) PhosphoSitePlus: a comprehensive resource for investigating the structure and function of experimentally determined post-translational modifications in man and mouse. *Nucleic Acids Res.* **40**, D261–D270
30. Smith-Garvin, J. E., Koretzky, G. A., and Jordan, M. S. (2009) T cell activation. *Annu. Rev. Immunol.* **27**, 591–619
31. Trickett, A., and Kwan, Y. L. (2003) T cell stimulation and expansion using anti-CD3/CD28 beads. *J. Immunol. Methods* **275**, 251–255
32. Gosling, K. M., Makaroff, L. E., Theodoratos, A., Kim, Y.-H., Whittle, B., Rui, L., Wu, H., Hong, N. A., Kennedy, G. C., Fritz, J.-A., Yates, A. L., Goodnow, C. C., and Fahrer, A. M. (2007) A mutation in a chromosome condensin II subunit, kleisin beta, specifically disrupts T cell development. *Proc. Natl. Acad. Sci. U. S. A.* **104**, 12445–12450
33. Rawlings, J. S., Gatzka, M., Thomas, P. G., and Ihle, J. N. (2011) Chromatin condensation via the condensin II complex is required for peripheral T-cell quiescence. *EMBO J.* **30**, 263–276
34. Yuen, K. C., Slaughter, B. D., and Gerton, J. L. (2017) Condensin II is anchored by TFIIIC and H3K4me3 in the mammalian genome and supports the expression of active dense gene clusters. *Sci. Adv.* **3**, e1700191